Ab initio study of the early stages of gas-phase water oxidation of the Si(100) (2 × 1):H surface

R. Lelis-Sousa* and M. J. Caldas†

Instituto de Física, Universidade de São Paulo, Rua do Matão, Travessa R 187, CEP 05508-900 São Paulo, Brazil

(Received 28 June 2011; revised manuscript received 25 October 2011; published 16 November 2011)

We investigate different reaction mechanisms for the dissociation of a H_2O molecule on the Si(100)(2 × 1):H surface, through *ab initio* calculations within density functional theory, comparing results using local density and generalized gradient approximations for the exchange-correlation potential. The reaction pathways were obtained with the "climbing image–nudged elastic band" procedure. In all cases we present complete analysis of the transition barriers and binding energies. Our results indicate that the oxidation route suggested by earlier works, which entails full chemisorption of the water molecule, is not favorable, and we propose two alternative routes with simultaneous release of one H_2 molecule.

DOI: 10.1103/PhysRevB.84.205314 PACS number(s): 68.43.Bc, 68.47.Fg, 82.20.Wt, 82.65.+r

I. INTRODUCTION

Oxidation of silicon surfaces has been a frequent object of study since the beginning of device physics and continues to receive careful attention,[1–3] especially due to the advances in nanoscience and molecular electronics.[4–6] Oxidation can come by exposure to molecular O_2 gas, to ambient air, or to water, and in the last two cases it is important to understand the initial reaction with water molecules. We are interested here in water oxidation of the monohydrogenated Si(100)(2 × 1):H, of relevance to hybrid organic-on-Si interfaces.[6,7]

The reaction of water with Si(100) surfaces has long been investigated, from the experimental and theoretical points of view,[8–32] and despite these efforts, there are still several open questions. For clean Si(100) surfaces it is agreed from the experimental results that, after interaction with water, almost 100% of the surface consists of very stable HSi– SiOH species[11–25,33,34] and the dimer-row pattern is maintained. In this case, theoretical studies find that the reaction proceeds without barrier.[17,33,35] As for hydrogen passivated Si(100):H surfaces, even though there are fewer experimental or theoretical studies of wet oxidation, analyses of infrared (IR) spectra confirm that they are more resistant to oxidative damage.[18–20,36,37] Monohydrogenated Si(100)(2 × 1):H reconstruction is very stable[38] and allows for the growth of samples with a high degree of homogeneity, which makes it an interesting substrate for applications in hybrid devices;[5–7] on the other hand, oxygen is known to be very important for determining surface reactivity (in fact some techniques rely specifically on using suboxides[4]), and since many approaches to the assembling of organic layers are based on wet-chemistry techniques, a thorough investigation of the early stages of oxidation by water of this particular surface is, therefore, very useful and motivates this work.

From a joint experimental and theoretical study[18–20] of the Si(100):H surface, based on IR spectroscopy and *ab initio* cluster-based simulations for vibrational modes, it has been proposed that, in the initial stages of oxidation, insertion of the water molecule occurs with dissociation as a silanol (SiOH) group and dimer-bond breaking (HSi-SiH + H_2O → HSiH + HSiOH). It is well established that increasing the water flux on a Si(100):H surface results in the disappearance of the IR signal for the pure surface dimer HSi-SiH and gives rise to vibrational peaks related to oxidized structures; however, the silanol vibrational modes at 821 and 2081 cm^{-1}, present for oxidation of the clean surface, were not identified in the experimental data. At advanced stages of wet oxidation, the IR signal is dominated by peaks located at 962–979 and 2143 cm^{-1} that, based on the calculations for the vibrational frequencies, were attributed to the presence of neighbor dihydrogenated surface groups, both clean HSiH and with a back-bond oxygen HSi(O)H (here we label this structure C_{BB}). These results suggest that the back bond is the main site for oxygen chemisorption.[18–20,26] Still according to this experimental interpretation,[18–20,26] oxidation of the back bond would follow from a HSiH + HSiOH precursor (we label this complete structure C_{Sil}).

An intriguing point is that at early stages of wet oxidation (data for a water exposure of 100 L),[18–20] the IR spectrum consists mainly of vibrational peaks in the ranges 803 to ≈870, ≈897 to 910, and 2120 cm^{-1}[20], and the frequencies for oxidized HSiH units (close to 962–979 cm^{-1}) are not identified. Indeed, the theoretical simulations[14,18–20] suggest instead oxidized dimer species HSi-O-SiH or HSi-Si(O)H, including multiply oxidized groups such as HSi-O-Si(O)H.

To our knowledge, issues related specifically to the interaction between a water molecule and HSi-SiH groups have not yet been discussed in the literature. We present here a theoretical investigation of energy barriers, transition states, and reaction pathways related to oxygen insertion in the Si(100)(2 × 1):H first subsurface region, at early stages of wet oxidation. We show that the C_{Sil} species will be formed on the surface, but the energy barrier for conversion into C_{BB} is very high, implying that silanol is not an effective route for oxygen insertion in subsurface sites. We propose two efficient routes for initial oxidation without dimer-bond breaking, one regarding oxidation of the back-bond site and another for on-dimer oxidation, which have favorable dissociation routes; both occur with simultaneous release of a H_2 molecule, producing HSi-O-SiH + H_2 (C_{OD}) and HSi-Si(O)H + H_2 (C_{BB+H2}) species. Again, to our knowledge, these structures have never been previously considered. An interesting result of our simulations is that silanol is actually a precursor not of the back-bond configuration, but of the on-dimer oxidation.

II. METHODOLOGY

The unit cell of the ideal Si(100)(2 × 1):H surface consists of two Si atoms per layer, with the surface dimers saturated

with H-forming symmetric HSi-SiH groups.[36,37,39] This ideal surface is modeled here by a periodic slab supercell, with six Si layers and (2×1):H reconstruction at both sides, separated by a vacuum layer of $\approx$19 Å. Only one side of this slab is reacted, with one water molecule. The minimum lateral periodicity we used was (2×2), and for specific cases we extended the simulations also to (2×4) and (4×3) surface unit cells.

The first principles reaction paths, energy barrier heights, and geometries for the transition states were obtained using the method known as climbing image–nudged elastic band (CI-NEB).[40] This method allows one to obtain the minimum energy path (MEP) between previously optimized initial and final states. For that, the reaction path is discretized with "images connected with a spring."[40] During the convergence procedure, only the initial and final states are kept frozen, while the other images of the "elastic band" move according to the constraints: system and elastic band. The MEP is found when the component of the force perpendicular to the "band" is null, while the parallel component dictates the relative position of the image.

As mentioned, we need, to start the procedure, optimized initial and final configurations. We used classical molecular dynamics (impact-CMD) within the PCFF (COMPASS)[41,42] empirical force field to choose the initial configurations. We used large lateral (8×6) unit cells and simulated the deposition of one single water molecule per trial. PCFF is not a reactive field, thus we only selected from these trials the most frequently found deposition sites. We identified different sites, shown in Fig. 1: one over the surface dimer, which we call P1; and another in the valley, P2. These structures were then optimized with DFT keeping the oxygen atom z coordinate fixed (distance from the surface). The final configurations, discussed in Sec. I, were taken from the experimental literature[12–14,20,21,26]—inserted as SiOH (C_{Sil}), in the back bond (C_{BB} and C_{BB+H2}), and on dimer (C_{OD})—and the optimized geometries for each structure were again obtained through DFT (Fig. 2). Emphasizing what was stated earlier, the C_{BB+H2} and C_{OD} structures had never been considered as possible products of oxidation of Si surfaces.

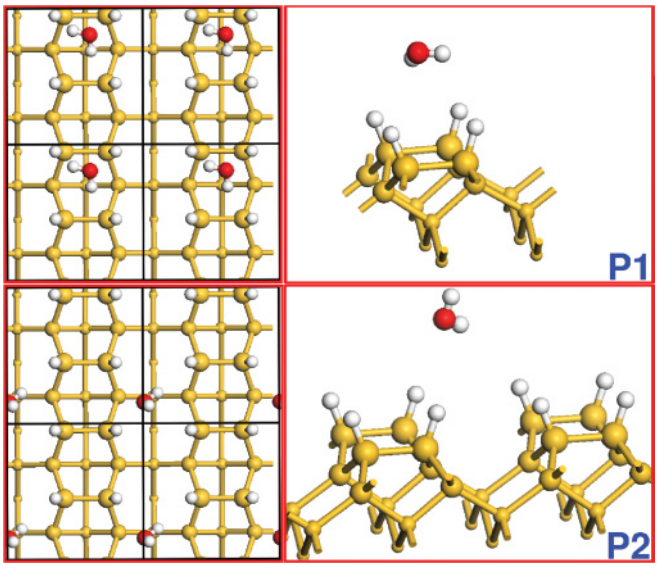

FIG. 1. (Color online) Top and side views of the DFT optimized (see text) configurations for the initial situations, in the smaller unit cell (2×2): over the dimer row, P1 (top panel); and over the valley, P2 (bottom panel). O atoms are shown in red, H atoms in white, and Si atoms in yellow. The size of yellow spheres is related to the Si position in the slab; the unit cell used in our *ab initio* simulations is indicated by black lines.

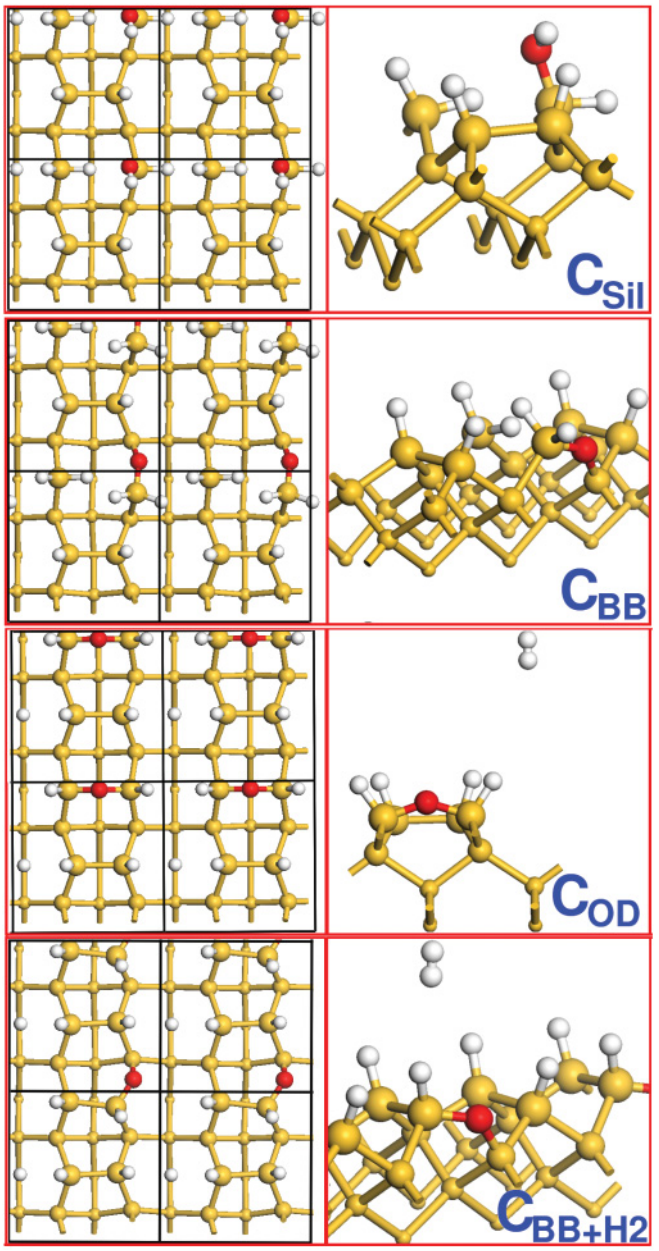

FIG. 2. (Color online) Top and side views of DFT optimized configurations for chemisorbed situations: C_{Sil}, C_{BB}, C_{OD}, and C_{BB+H2}. O atoms are shown in red, H atoms in white, and Si atoms in yellow. The size of yellow spheres is related to the Si position in the slab used in our simulation; the unit cell used in our *ab initio* simulations is indicated by black lines.

DFT calculations were performed using the plane-wave pseudopotential implementation QUANTUM ESPRESSO,[43] within both approximations—local density, as parametrized by Perdew and Zunger (LDA-PZ);[44,45] and generalized

TABLE I. Binding energy ΔE (eV/molecule) for physisorbed P (initial) and chemisorbed C (final) structures (Figs. 1 and 2), and interatomic distance (Å) between nearest Si and O neighbors for the initial configurations.

	P1	P2	C_{Sil}	C_{BB+H2}	C_{BB}	C_{OD}
ΔE_{LDA}	−0.04	−0.03	−0.71	−0.61	−1.11	−1.18
ΔE_{GGA}	−0.03	−0.03	−0.55	−0.87	−1.13	−1.43
R_{Si-O} (Å)	4.67	4.80	—	—	—	—

gradient (GGA-PW91)[46]—for the exchange-correlation functional. Comparison of results from the two functionals allows one to obtain a better estimate of barrier heights. We used, in all cases, ultrasoft pseudopotentials[47] for core electron simulation, except for the Si atom in the LDA calculations, in which case we used a norm-conserving pseudopotential.[48] This allowed us to use a 25-Ry energy cutoff for plane waves and 250 Ry for electronic densities. For the (2×2) unit cell the DFT equations were solved with 10 special k points in the Monkhorst-Pack[49] scheme. The convergence criterion for geometry optimization was 0.025 eV Å^{-1}, and for the reaction path, MEP convergence for the perpendicular force was 0.09 eV Å^{-1}. Binding energies were obtained by taking the difference between the total energy of the final and that of initial structures including all components.

III. RESULTS

We discuss first the chosen initial and final configurations. The DFT optimized structures for the two initial configurations P1 and P2 are shown in Fig. 1, and we summarize in Table I the binding energies obtained, as well as the relevant Si-O distances. As we see, the *ab initio* results indicate that, in both cases, the water molecule is physically adsorbed on the surface; additionally, the binding energy for the configuration P1 does not change when we use the larger (4×4) unit cell, and we expect this to be true also for the P2 configuration. The low values of the binding energies, however, do not allow us to distinguish them by stability. The *ab initio* relaxed structures for the final configurations are illustrated in Fig. 2 and their respective binding energies are also listed in Table I. Our calculations (LDA or GGA) show that C_{OD} is more stable than all the other configurations. Of all species studied, the C_{Sil} is the least stable chemisorbed situation according to our GGA results, in agreement with previous theoretical data.[26,50] In the case of LDA results, C_{BB+H2} is slightly less stable than C_{Sil}. We now discuss our results for the reactions leading from P1 or P2 to all of the above final configurations.

A. Insertion as silanol

We start with the MEP, followed by the system to go from P1 to C_{Sil}, calculated with LDA and GGA; this reaction is illustrated in Fig. 3, where we show the variation of the energy landscape as a function of the "distance between images" used in the construction of the "elastic band." The zero of the energy scale coincides with the sum of the energies for the isolated subsystems [isolated water molecule and Si(100)(2×1):H]. We also included some images for the relevant configurations:

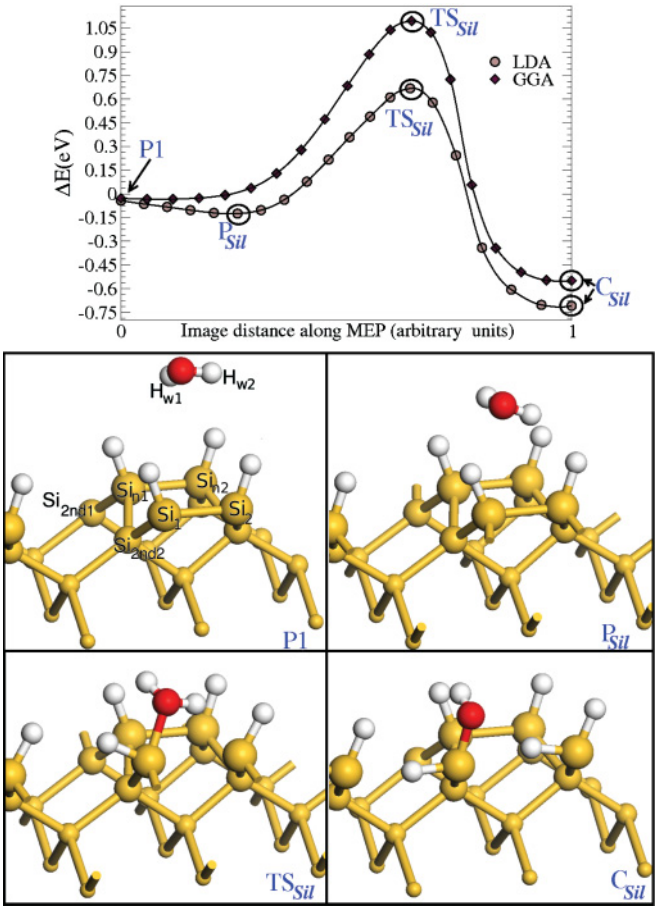

FIG. 3. (Color online) Top: Minimum energy path (MEP) for H_2O dissociation on Si(100)(2×1):H as C_{Sil} obtained with LDA (circles) and GGA (rhombuses) calculations; lines are a guide for the eye. Bottom: Geometric structures of special path points (images): starting point (P1), physisorbed configuration (P_{Sil}), transition state (TS_{Sil}), and final chemisorbed configuration (C_{Sil}). The 0 on the energy scale was set to the energy for isolated subsystems [isolated H_2O molecule and Si(100)(2×1):H surface] for each of the functionals.

starting point (P1), physisorbed (P_{Sil}), transition state (TS_{Sil}), and final chemisorbed configuration (C_{Sil}). In this case, we emphasize that all geometric configurations for this reaction are essentially the same for either LDA or GGA calculations; that is, the system follows the same reaction path (Table II). There are significant differences in the *energy profile* calculated with the different functionals. First, the LDA result predicts that the C_{Sil} species is 0.16 eV more stable on the surface than what was obtained with GGA simulations. Second, we notice that, even if the P_{Sil} geometric configuration is in the GGA path, it is not a physisorbed situation, as predicted by LDA. Third, the energy barrier which the system has to overcome to produce the SiOH unit is ≈0.3 eV lower from the LDA results compared to the GGA (Table III).

At this point, it is interesting to compare the present results with our previous study of wet oxidation of clean Si(100)(2×1) surfaces.[33] We have shown that there is no barrier to water dissociation on the clean surface, and the HSi-SiOH species is formed with an energy gain of $\Delta E = 2.52$ eV. Here, on the monohydride surface, we find that the water

TABLE II. Interatomic distances for chosen configurations of the indicated MEPs (see Figs. 3 and 4). Distances in angstroms; results obtained with LDA (GGA).

	Si(100)	P1	P1 → C_{Sil}		C_{Sil} → C_{BB}		C_{BB}
	(2 × 1):H		TS_{Sil}	C_{Sil}	TS_{1Sil} → BB	TS_{2Sil} → BB	
Si_1-Si_2	2.41 (2.44)	2.41 (2.44)	3.03 (3.12)	3.94 (4.01)	4.01 (4.18)	4.22 (4.29)	4.00 (4.04)
H_{w1}-O	—	0.97 (0.98)	0.99 (0.99)	0.98 (0.97)	1.76 (2.11)	2.51 (2.60)	2.59 (2.60)
H_{w2}-O	—	0.98 (0.97)	1.02 (1.02)	2.40 (2.47)	2.29 (2.62)	2.17 (2.31)	2.72 (2.77)
O-Si_1	—	4.66 (4.64)	1.95 (1.97)	1.67 (1.67)	1.57 (1.56)	1.61 (1.60)	1.66 (1.66)
O-Si_2	—	4.66 (4.78)	3.01 (3.06)	3.84 (3.90)	3.78 (4.12)	3.57 (3.65)	4.08 (4.11)
O–Si_{2nd1}	—	—	3.85 (3.88)	3.36 (3.39)	3.55 (3.57)	2.25 (2.23)	1.67 (1.67)
Si_1-H_{w1}	—	—	2.54 (2.54)	2.29 (2.28)	1.70 (1.78)	1.71 (1.71)	1.49 (1.49)
H_{w1}-Si_{2nd2}	—	—	3.82 (3.81)	3.60 (3.59)	1.65 (2.77)	1.57 (1.57)	3.16 (3.20)

molecule has to overcome a high energy barrier to form C_{Sil}, in good agreement with the experimental fact that hydrogen passivation hinders the wet oxidation of silicon surfaces. Experimental results, in fact, indicate that the water molecule has a high sticking coefficient on clean surfaces,[18–20,24] and under the same conditions the oxidation of Si(100)(2 × 1):H occurs but is limited. We find that oxygen incorporation as C_{Sil} proceeds through a transition state (TS_{Sil}) in which the oxygen atom has three asymmetric bonds, and one surface silicon atom has a dangling bond (since the Si_1-Si_2 bond does not exist anymore). Another interesting result is that the energy barrier for production of C_{Sil} does not depend on the initial position of the water molecule: we find the same activation energy starting the reaction from the P1 or P2 configuration (Tables III and IV).

Proceeding, we report in Table III the energy barrier heights obtained with the LDA and GGA functionals for these MEPs, for both insertion and desorption. We see that the desorption barrier is high, that is, a water molecule will not be easily released back from the surface, and as such, we should expect to observe this defect on the surface. As we pointed out above, the usual suggestion[18–20] is that the silanol unit is actually, in any case, the initial oxidation step and is not seen in the surface because it converts to the surface unit on dimer or, as is more frequently supposed,[18,20,26] to the back bond. Let us now discuss our results for these conversion reactions.

TABLE III. Barrier heights (eV) for insertion (TS) and desorption (D) obtained for the systems shown in Figs. 3–6. All calculations were made using a (2 × 2) unit cell, except where indicated.

System	Barrier height	LDA (eV)	GGA (eV)
P1 → C_{Sil}	TS	0.792	1.122
	D	1.501	1.645
C_{Sil} → C_{BB}	TS1 (2 × 2)/(24)	2.412/2.303	—/2.186
	D1 (2 × 2)/(2 × 4)	0.516/0.472	—/0.560
	TS2 (2 × 2)/(2 × 4)	0.747/0.767	—/0.899
	D2 (2 × 2)/(2 × 4)	3.047/3.048	—/3.155
P2 → C_{BB+H2}	TS	0.699	1.027
	D (C'_{BB+H2})	1.067	1.924
	D (C_{BB+H2})	1.306	1.899
P1 → C_{OD}	TS_{Sil}	0.846	1.120
	D_{Sil}	1.538	1.604
	TS_{OD2}	0.372/0.470	0.472/0.529
	D (C'_{OD})	2.113	2.543
	D (C_{OD})	2.010	2.529

B. Silanol to back bond

Figure 4 shows the reaction MEP obtained with both LDA and GGA functionals, together with illustrations of the optimized configurations for the initial C_{Sil}, transition states $TS_{1Sil→BB}$ and $TS_{2Sil→BB}$, and final C_{BB}. Structural parameters are also summarized in Table II. We can check that, even if for this MEP at the transition states, the structural parameters may differ strongly from LDA to GGA, this does not happen for the chemisorbed configurations C_{Sil} and C_{BB}.

We see from Fig. 4 and the values in Table III that the energy barrier for this process is very high. To investigate whether this result was a consequence of the small unit cell used in our simulation, we extended the calculation using a (2 × 4) unit cell. Comparison of these results demonstrates that the MEP is not sensitive to the enlargement of the unit cell. Once C_{BB} is formed, the desorption energy is high enough to prevent any back reaction, however, the process is not straightforward. The conversion of C_{Sil} to C_{BB} passes through two transition states,

TABLE IV. Barrier heights (eV) for insertion (TS) and desorption (D) obtained for the indicated system. All calculations were made using a (2 × 2) unit cell, except where indicated.

System	Barrier height	LDA (eV)
P2 → C_{Sil}	TS	0.794
	D	1.502
C_{Sil} → C_{BB}	TS1-A	2.751
	D1-A	2.881
	TS2-A	0.815
	D2-A	1.090
C_{BB+H2} → C_{BB}	TS	1.969
	D	2.378
C_{OD} → $C_{OD+SiH2}$	TS (4 × 3)	2.245
	D (4 × 3)	3.971
C_{OD} → C_{BB}	TS	2.289
	D	2.673

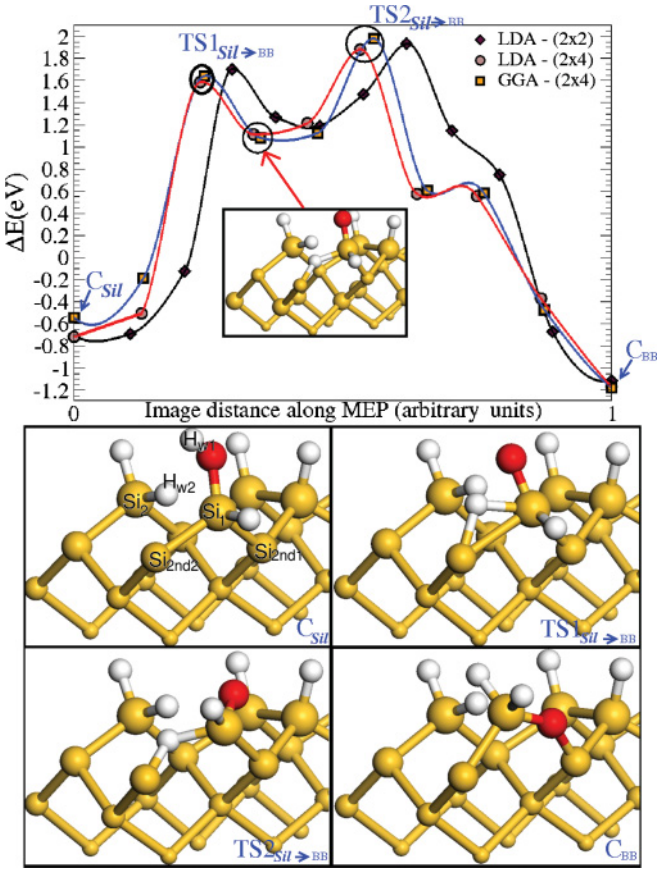

FIG. 4. (Color online) Top: MEP for silanol (C_{Sil}) conversion to back bond (C_{BB}) obtained with LDA and GGA calculations using (2 × 2) unit cells (LDA; rhombuses) and (2 × 4) unit cells (LDA, circles; GGA, squares); lines are a guide for the eye. Bottom: Geometric structures of special path points (images): starting point (C_{Sil}), first transition state ($TS1_{Sil\to BB}$), intermediate (inset), second transition state ($TS2_{Sil\to BB}$), and final chemisorbed configuration (C_{BB}). The 0 on the energy scale was set to the energy for isolated subsystems [isolated H_2O molecule and Si(100)(2 × 1):H surface] for each of the functionals.

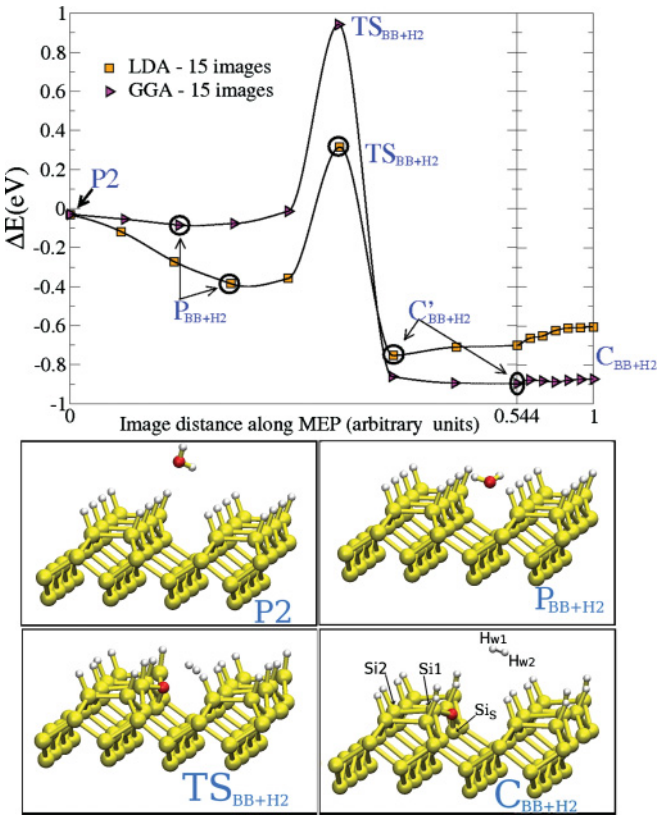

FIG. 5. (Color online) Top: MEP for back-bond oxidation of Si(100)(2 × 1):H as H_2O dissociation with release of one H_2 molecule C_{BB+H2} obtained with LDA (squares) and GGA (triangles) calculations; lines are a guide for the eye. Bottom: Geometric structures of special path points (images): starting point (P2), physisorbed configuration (P_{BB+H2}), transition state (TS_{BB+H2}), and final chemisorbed configuration (C_{BB+H2}). The 0 on the energy scale was set to the energy for isolated subsystems [isolated water molecule and Si(100)(2 × 1):H surface] for each of the functionals. From image 9 onward (compressed) the only difference concerns the distance of the H_2 molecule from the surface.

with an intermediate state. The first energy barrier is associated with the breaking of the OH bond of the silanol unit (TS1, $C_{Sil} \to C_{BB}$), needed for insertion of the O atom: the system relaxes to a lower energy state, in which that H atom moves to the first subsurface, while the distance Si-O approaches that found for silanone structures.[30] As a consequence of the small barrier for desorption ($\Delta E_{LDA} = +0.47$ eV and $\Delta E_{GGA} = +0.56$ eV), there is a reasonable probability that, at this intermediate configuration, the system reverts back to C_{Sil} to form C_{BB} the system needs to overcome the second barrier, related to insertion of the oxygen atom at the back-bond

TABLE V. Interatomic distances for chosen configurations of the MEP shown in Fig. 5: initial (P2), transition (TS_{BB+H2}), C'_{BB+H2}, and final (C_{BB+H2}) configurations. Distances in angstroms; results obtained with LDA (GGA).

	P2	C → C_{BB+H2}			
		P_{BB+H2}	TS_{BB+H2}	C'_{BB+H2}	C_{BB+H2}
H-Si	1.50 (1.50)	1.51 (1.50)	1.48 (1.47)	1.50 (1.50)	1.50 (1.50)
Si_1-Si_2	2.42 (2.44)	2.41 (2.43)	2.51 (2.61)	2.42 (2.44)	2.42 (2.44)
O-Si_1	4.83 (4.79)	3.49 (3.63)	1.72 (1.78)	1.66 (1.67)	1.66 (1.66)
O-Si_S	5.47 (5.44)	3.27 (3.74)	1.71 (1.74)	1.68 (1.68)	1.68 (1.68)
O-H_{w1}	0.98 (0.97)	0.98 (0.98)	2.12 (2.03)	2.24 (2.62)	6.69 (6.75)
O-H_{w2}	0.98 (0.98)	0.98 (0.97)	2.31 (2.29)	2.98 (3.37)	7.36 (7.40)
H_{w1}-H_{w2}	1.55 (1.54)	1.58 (1.54)	0.79 (0.78)	0.77 (0.75)	0.77 (0.75)

site, with a higher energy. It should be noted that we also investigated another possible route for the conversion of C_{Sil} into C_{BB}, but the energy barrier for this process (TS1-A, $C_{Sil} \rightarrow C_{BB}$; reported in Table IV) is higher.

We also calculated MEPs for several alternative reaction paths for the back-bond oxidation with complete absorption of the water molecule components, for instance, starting from the P2 configuration, but the energy barriers are even higher (reaching about 3 eV). Therefore, due to the complex kinetic properties (Fig. 4) and high barriers, it is difficult to propose this reaction under experimental conditions (wet oxidation occurs already at 300 K).[18–20]

C. Backbond insertion with release of H_2

We thus turned to a different strategy, investigating reactions that assume release of a H_2 molecule. The best path we found, leading to C_{BB+H2}, starts from P2, that is, with the initial configuration for the water molecule over the valley. We show in Fig. 5 the energy profile along the reaction path with both LDA and GGA functionals. We see that the activation energy for the production of C_{BB+H2} is now slightly lower than that of complete insertion as C_{Sil} (LDA or GGA; MEP shown in Fig. 3).

A distinctive feature of the reaction of water with a monohydrogenated Si surface is shown in Fig. 5. According to both LDA and GGA results, there is a physisorbed situation P_{BB+H2} with an energy gain of $\Delta E = 0.35$ eV for LDA ($\Delta E = 0.08$ eV for GGA), in which the H atoms from the water molecule are "attracted" by the surface H atoms (structural parameters are listed in Table V). This is related to the negative charge of the H atoms in HSi-SiH units. After the transition state, before release of the H_2 molecule, there is again an almost-stable configuration for this molecule (C'_{BB+H2}). We also investigated the possibility of H_2 molecule dissociation from this point, with saturation of the closest dimer. As reported in Table IV, the energy barrier (TS; $C_{BB+H2} \rightarrow C_{BB}$) is enough to prevent this process under the experimental conditions.

In summary, the critical information provided by the results in Figs. 3 and 5, and Table III, is that direct oxidation of the back bond, but with release of a H_2 molecule, is more realistic than the proposal of silanol as the intermediate state.

D. Dimer oxidation with release of H_2

We now turn to the results for dimer oxidation starting from the P1 configuration. In this case the MEP passes through two transition states, TS_{Sil} and TS_{OD2} (Fig. 6), that is, the reaction must start through the formation of a silanol structure—-and we never imposed this kind of constraint on the calculation. Structural parameters for transitions and chemisorbed configurations are reported in Table VI. Contrary to the high value for the silanol desorption barrier, only a low energy barrier (Table III; energy barrier TS_{OD2}) must be overcome to complete the oxygen insertion at the on-dimer site. Since the configuration for C_{Sil} inside the MEP is not exactly the same as the one we obtain with full relaxed optimization, we recalculated part of the reaction path, starting now from the optimized C_{Sil} configuration, and the energy

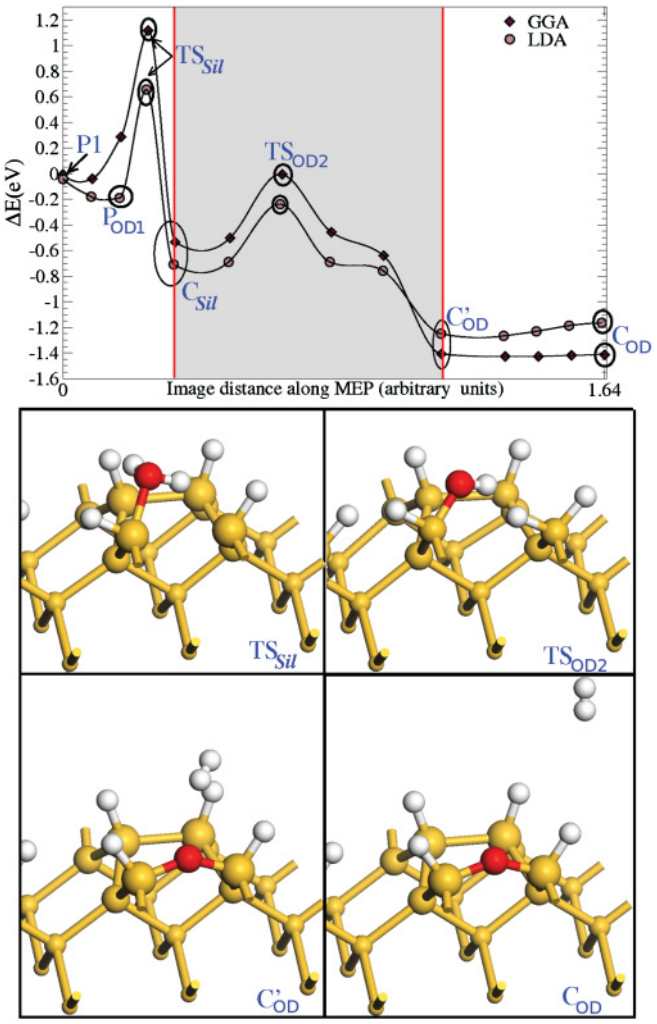

FIG. 6. (Color online) Top: MEP for on-dimer oxidation of Si(100)(2 × 1):H as H_2O dissociation with release of one H_2 molecule, C_{OD}, obtained with LDA (circles) and GGA (rhombuses) calculations; lines are a guide for the eye. Bottom: Geometric structures of special path points (images): starting point (P1), first transition state (TS_{Sil}), second transition state (TS_{OD2}), C'_{OD}, and final chemisorbed configuration (C_{OD}). The zero of the energy scale was set to the energy for isolated subsystems [isolated H_2O molecule and Si(100)(2 × 1):H surface] for each of the functionals. The images in the shaded area come from the refined calculations (see text).

barriers are very similar (this refined calculation is shown in the shaded area in Fig. 6). Also, here we identified a geometric conformation C'_{OD} in which the H_2 molecule is attracted by the surface (see Fig. 6 and Table VI): we thus investigated whether the H_2 molecule could move toward to the neighbor dimer and produce two dihydrogenated HSiH units, and again, our results indicate that the energy barrier (TS; $C_{OD} \rightarrow C_{OD+SiH2}$) is rather high (Table IV). Analyzed together, these factors ensure that once C_{Sil} is produced, there is a high probability that C_{OD} will be formed.

Our simulations point to a different interpretation of the experimental data, since the path passes through the silanol configuration. According to our results, we propose that although the presence of C_{Sil} species is not clear in IR measurements,[18–20] this does not mean that they are not

TABLE VI. Interatomic distances for chosen configurations of the MEPs shown in Fig. 6: transition (TS_{OD2}) and final (C'_{OD} and C_{OD}) configurations. We include structural parameters calculated for the structures TS_{OD2} and C'_{OD}, obtained from two different NEB simulations: the first calculation covers the P1 configuration to the final image C_{OD}; for the second calculation we refine the MEP simulation covering C_{Sil} to C'_{OD}. This refined reaction path is represented in the shaded area in Fig. 6. Distances in angstroms; results obtained with LDA (GGA).

	$P1 \rightarrow C_{OD}$			$C_{Sil} \rightarrow C'_{OD}$	
	TS_{OD2}	C'_{OD}	C_{OD}	TS_{OD2}	C'_{OD}
H-Si	1.50 (1.50)	1.50 (1.50)	1.50 (1.50)	1.50 (1.50)	1.50 (1.50)
Si_1-Si_2	3.88 (3.90)	3.17 (3.17)	3.17 (3.17)	3.87 (3.92)	3.17 (3.17)
H_{w1}-O	0.98 (0.97)	2.62 (4.42)	7.43 (7.45)	0.98 (0.97)	4.51 (4.42)
H_{w2}-O	2.11 (2.10)	3.36 (4.93)	7.95 (7.98)	2.21 (2.25)	5.06 (4.93)
O-Si_1	1.67 (1.67)	1.67 (1.67)	1.67 (1.67)	1.68 (1.68)	1.67 (1.67)
O-Si_2	3.36 (3.42)	1.67 (1.67)	1.67 (1.67)	3.06 (3.09)	1.67 (1.67)
H_2-surface	—	2.62 (2.41)	4.80 (4.78)	—	2.34 (2.41)

produced. Actually, our simulations are consistent with the hypothesis that SiOH groups are being formed, but transformed in other oxidized species, which we propose to be on dimer, C_{OD}. Evidence in support of this interpretation is afforded by the same IR data since the calculation of vibrational modes[14,18–20] predicts multiply oxidized species, which can only be achieved through release of H_2 molecules.

Finally, we investigated also whether the back-bond configuration could be reached from this on-dimer oxidation, but the energy barrier for this process is as high as that calculated to produce C_{BB} from C_{Sil} (data included in Tables III and IV), thus we conclude that C_{OD} is not easily converted to C_{BB}.

IV. SUMMARY AND CONCLUSIONS

We have investigated the dissociation of a water molecule on the Si(100)(2 × 1):H surface using *ab initio* methods, with analysis of the possible reaction paths, and using different functionals. We observe that the main barriers and intermediate local minima in the reaction paths are the same for both functionals, and thus the general conclusions are not affected by the choice of approximation. However, it is to be noted that, apart from the general trend for the height obtained with the GGA (expected to be higher than that with the LDA), there is no reasonable procedure to estimate a correction to the barrier height obtained from one functional that could lead to the value obtained from the other.

As a general conclusion, we did not find any reaction path that could lead to wet oxidation of the first surface layer without a barrier. Among the considered reactions, that with the lowest barrier leads to back-bond oxidation of the surface, with release of a H_2 molecule. The next reaction that follows closely in energy is the formation of a silanol unit: however, once this unit is formed, there is a high probability that it will result in surface on-dimer oxidation, again with the release of a H_2 molecule.

These results are in agreement with the interpretation of infrared results[18–20,26] that point to the presence of multiply oxidized surface units and, also, with the assumption of the presence of silanol surface units in the very early stages of wet oxidation.

ACKNOWLEDGMENTS

We acknowledge support from the Brazilian agencies CAPES, FAPESP and CNPq, as well as Ministry of Science and Technology grants IN, IMMP, and INEO, and the use of computational facilities at LCCA-USP and CENAPAD-SP.

*Corresponding author: rlsouza@if.usp.br; Present Address: Departamento de Ciências Naturais, Licenciatura em Física, Universidade Federal do Tocantins, Campus de Araguaína, Rua Paraguai S/N, CEP 77824-838, Araguaína, Brazil.

†mjcaldas@usp.br

[1] L. Caramella, C. Hogan, G. Onida, and R. Del Sole, Phys. Rev. B **79**, 155447 (2009).

[2] K. Gaál-Nagy, A. Incze, G. Onida, Y. Borensztein, N. Witkowski, O. Pluchery, F. Fuchs, F. Bechstedt, and R. Del Sole, Phys. Rev. B **79**, 045312 (2009).

[3] L. Caramella, C. Hogan, G. Onida, and R. Del Sole, Phys. Status Solidi B **247**, 1946 (2010).

[4] N. Clement, S. Pleutin, D. Guerin, and D. Vuillaume, Phys. Rev. B **82**, 035404 (2010).

[5] A. Salomon, T. Boecking, C. K. Chan, F. Amy, O. Girshevitz, D. Cahen, and A. Kahn, Phys. Rev. Lett. **95**, 266807 (2005).

[6] M. A. Walsh, S. R. Walter, K. H. Bevan, F. M. Geiger, and M. C. Hersam, J. Am. Chem. Soc. **132**, 3013 (2010).

[7] C. S. Cucinotta, A. Ruini, E. Molinari, C. A. Pignedoli, A. Catellani, and M. J. Caldas, J. Phys. Chem. C **112**, 10167 (2008).

[8] L. Incoccia, A. Balerna, S. Cramm, C. Kunz, F. Senf, and I. Storjohann, Surf. Sci. **189**, 453 (1987).

[9] R. J. Hamers and Y. Wang, Chem. Rev. **96**, 1261 (1996).

[10] Y. J. Chabal and S. B. Christman, Phys. Rev. B **29**, 6974 (1984).

[11] K. Raghavachari, Y. J. Chabal, and L. M. Struck, Chem. Phys. Lett. **252**, 230 (1996).

[12] M. K. Weldon, B. B. Stefanov, K. Raghavachari, and Y. J. Chabal, Phys. Rev. Lett. **79**, 2851 (1997).

[13] B. B. Stefanov, A. B. Gurevich, M. K. Weldon, K. Raghavachari, and Y. J. Chabal, Phys. Rev. Lett. **81**, 3908 (1998).

[14] M. K. Weldon, K. T. Queeney, A. B. Gurevich, B. B. Stefanov, Y. J. Chabal, and K. Raghavachari, J. Chem. Phys. **113**, 2440 (2000).

[15]L. M. Struck, J. E. Jr., B. E. Bent, G. W. Flynn, Y. J. Chabal, S. B. C. E. E. Chaban, K. Raghavachari, G. P. Willians, K. Radermacher, and S. Mantl, Surf. Sci. **380**, 444 (1997).
[16]A. Estève, Y. J. Chabal, F. Raghavachari, M. K. Weldon, K. T. Queeney, and M. D. Rouhani, J. Appl. Phys. **90**, 6000 (2001).
[17]K. T. Queeney, M. K. Weldon, Y. J. Chabal, and K. Raghavachari, J. Chem. Phys. **119**, 2307 (2003).
[18]G. R. Rao, Z.-H. Wang, H. Watanabe, M. Aoyagi, and T. Urisu, Surf. Sci. **570**, 178 (2004).
[19]Z.-H. Wang, T. Urisu, S. Nanbu, J. Maki, G. R. Rao, M. Aoyagi, H. Watanabe, and K. Ooi, Phys. Rev. B **69**, 045309 (2004).
[20]Z.-H. Wang, T. Urisu, H. Watanabe, K. Ooi, G. R. Rao, S. Nanbu, J. Maki, and M. Aoyagi, Surf. Sci. **575**, 330 (2005).
[21]H. Watanabe, S. Nanbu, Z.-H. Wang, and M. Aoyagi, Chem. Phys. Lett. **424**, 133 (2006).
[22]B. R. Trenhaile, A. Agrawal, and J. H. Weaver, Appl. Phys. Lett. **89**, 151917 (2006).
[23]S.-Y. Yu, H. Kim, and J.-Y. Koo, Phys. Rev. Lett. **100**, 036107 (2008).
[24]H. N. Waltenburg and J. T. Yates, Chem. Rev. **95**, 1589 (1995).
[25]L. Andersohn and U. Kohler, Surf. Sci. **284**, 77 (1993).
[26]H. Watanabe, S. Nanbu, Z.-H. Wang, J. Maki, T. Urisu, M. Aoyagi, and K. Ooi, Chem. Phys. Lett. **383**, 523 (2004).
[27]D. B. Skliar and B. G. Willis, J. Phys. Chem. C **112**, 9434 (2008).
[28]Y. Miyamoto, Phys. Rev. B **46**, 12473 (1992).
[29]T. Uchiyama and M. Tsukada, Phys. Rev. B **55**, 9356 (1997).
[30]Y. J. Chabal, K. Raghavachari, X. Zhang, and E. Garfunkel, Phys. Rev. B **66**, 161315 (2002).
[31]S. Okano and A. Oshiyama, Surf. Sci. **554**, 272 (2004).
[32]O. Warschkow, S. R. Schofield, N. A. Marks, M. W. Radny, P. V. Smith, and D. R. McKenzie, Phys. Rev. B **77**, 201305 (2008).
[33]R. Lelis-Sousa and M. J. Caldas, AIP Conf. Proc. **1199**, 9 (2010).
[34]C. Fan and G. Lopinski, Surf. Sci. **604**, 996 (2010).
[35]R. D. Smardon and G. P. Srivastava, Surf. Sci. **584**, 161 (2005).
[36]J. J. Boland, Phys. Rev. Lett. **65**, 3325 (1990).
[37]J. J. Boland, Surf. Sci. **261**, 17 (1992).
[38]S. Brueckner, H. Doescher, P. Kleinschmidt, and T. Hannappel, Appl. Phys. Lett. **98**, 211909 (2011).
[39]Y. Wang, M. J. Bronikowski, and R. J. Hamers, J. Vac. Sci. Technol. A **12**, 2051 (1994).
[40]G. Henkelman, B. P. Uberuaga, and H. Jósson, J. Chem. Phys. **113**, 9901 (2000).
[41]H. Sun, J. Phys. Chem. B **102**, 7338 (1998).
[42]M. J. Hwang, T. P. Stockfish, and A. T. Hagler, J. Am. Chem. Soc. **116**, 2515 (1994).
[43]P. Gianozzi *et al*., J. Phys. Condens. Matter **21**, 395502 (2009).
[44]D. M. Ceperley and B. J. Alder, Phys. Rev. Lett. **45**, 566 (1980).
[45]J. P. Perdew and A. Zunger, Phys. Rev. B **23**, 5048 (1981).
[46]J. P. Perdew and Y. Wang, Phys. Rev. B **33**, R8800 (1986).
[47]D. Vanderbilt, Phys. Rev. B **41**, 7892 (1990).
[48]N. Troullier and J. L. Martins, Phys. Rev. B **43**, 1993 (1991).
[49]H. J. Monkhorst and J. D. Pack, Phys. Rev. B **13**, 5188 (1976).
[50]R. J. Baierle and M. J. Caldas, Int. J. Mod. Phys. B **13**, 2733 (1999).